

# Wave-character preserving pre-stack map migration using curvelets

Huub Douma\* and Maarten V. de Hoop, Center for Wave Phenomena, Colorado School of Mines

## Summary

We treat the sparsification of the inverse scattering operator in the curvelet frame and state the conditions when such sparsification is feasible. Since common-offset (CO) Kirchhoff migration in the absence of caustics satisfies these conditions, we analyze the sparsity after such migration of a curvelet, and observe little leakage into neighboring curvelets, in both the spatial and spectral domains. This exemplifies the ability of curvelets to sparsify the imaging operator. In addition, we compare CO Kirchhoff time-migrated curvelets with CO map time-migrated curvelets, and show that map migration maps the indices of the unmigrated curvelets onto (or near) the indices of the largest coefficients of the migrated curvelets. This shows that map migration indeed provides the geometry of migration in the curvelet domain. Hence, we can devise a wave-character preserving map migration that essentially images the data in the compressed domain through a mapping of coefficients given by map migration. In essence, we present the CO time-migration variant of this. Hence, we lift the restriction of applicability of map migration beyond velocity model building, and show its use for fast imaging in the curvelet domain. Importantly, in our example, the curvelet CO map time-migration is almost two orders of magnitude faster than the CO Kirchhoff migration.

## Introduction

The slope information in seismic data, together with the velocity model, determine the directions of the recorded wavefronts. Map migration (Kleyn, 1977; Douma & de Hoop, 2003) explicitly uses this information to determine the reflector position and orientation in the image from surface seismic data. However, the wave character of the data is lost in map migration, which is based solely on traveltime picking. Hence, its main application, so far, has been in velocity model building (Gjoystdal & Ursin, 1981; Iversen *et al.*, 2000).

Recently, Hua and McMechan (2003) introduced parsimonious migration, which explicitly uses the slopes in common-source and common-receiver gathers to image the data pre-stack. The slopes are estimated using local slant stacks in these gathers, and rays are traced only in the associated directions. This results in a large reduction of computation time compared to, e.g., Kirchhoff methods, where many rays need to be traced to calculate the diffraction surfaces. In addition, an amplitude thresholding procedure aims to select the reflections, and thus further reduces computation time.

Like most existing migration algorithms, parsimonious migration images the data on a sample-by-sample basis. A sample-by-sample representation of the data, however, does not incorporate the *a priori* knowledge that a wavefield consists largely of a superposition of bandlimited, ori-

ented singularities (or reflections). It seems natural to attempt to represent seismic data with functions that have such character built into them. In this way, the slope information would be naturally built into the data representation, and would follow from a projection of the data onto these functions.

In the field of harmonic analysis, Candès and Guo (2002) and Candès and Donoho (2002) recently introduced a tight frame of (second-generation) curvelets, which provide an essentially optimal representation of objects that are twice continuously differentiable ( $C^2$ ) with discontinuities along  $C^2$  edges. Moreover, Candès and Demanet (2002) showed that these curvelets in essence optimally sparsify certain Fourier Integral Operators (FIO's). Since reflections in seismic data lie mainly along curves, and since our imaging operator is an FIO, curvelets should be plausible candidates for simultaneous compression of seismic data and the imaging operator. This was earlier also noted by Herrmann (2003).

This frame of curvelets is closely related to the frame introduced by Smith (1998). In fact, the elements in this frame are closely related to the notion of parabolic cutoff (Boutet de Monvel, 1974) that leads to a decomposition of FIO's into operators with amplitudes of type  $(1/2, 1/2)$ . (As a consequence, the amplitude aspects of imaging in the compressed domain are not straightforward.) A key condition here is that the canonical relation of the FIO is a canonical graph. In the absence of caustics, CO Kirchhoff migration satisfies this condition. In the presence of caustics, the usual scattering and imaging operators have to be extended to satisfy this condition.

Curvelets have direction built into them. This directional sensitivity, together with their spatial localization, suggests a close connection with map migration. As we show in this work, map migration provides the *mapping of the coefficients* from the curvelet decomposition of the seismic data to their migrated counterparts. This, combined with the oscillatory nature of curvelets, suggests that we can setup a pre-stack map migration that preserves wave character to image seismic data. This idea is somewhat related to parsimonious migration, where we replace the slant-stacking and amplitude thresholding parts with a curvelet decomposition of the data (followed by thresholding for denoising purposes). This decomposition both compresses the data and provides the slopes in the data, and hence allows imaging in the compressed domain using map migration.

Here we compare a map-migrated curvelet with a Kirchhoff-migrated curvelet, and show that map migration indeed provides the mapping from unmigrated to migrated curvelets. As an example we use 2D CO pre-stack time migration. We concern ourselves with the geometry of migration only, and defer the treatment of the amplitude aspects to a future paper, as this requires a technical analysis. Hence, strictly speaking, we treat the mapping of only the curvelet indices rather than the coefficients.

## Pre-stack map migration with curvelets

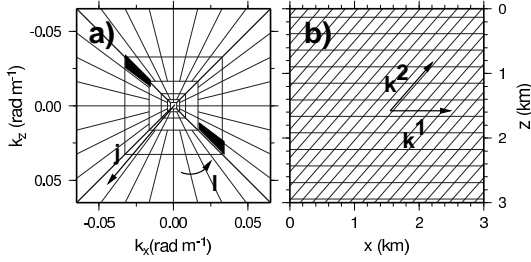


Fig. 1: Tiling of the spectrum (a) in the digital curvelet transform, and a particular dual tiling of 2D space (b) related to the shaded wedges in (a). The directions of increasing  $j$ ,  $l$ ,  $k^1$  and  $k^2$  are indicated with arrows.

i.e., a scale parameter ( $j = 0, 1, 2, \dots$ ), an orientation parameter ( $l = 0, 1, \dots, 2^{\lfloor j/2 \rfloor} - 1$ , where  $\lfloor x \rfloor$  indicates the integer part of  $x$ ), and translation parameters  $k^1$  and  $k^2$  (with  $k^1$  and  $k^2$  integers). In relation to seismic data,  $j$  and  $l$  determine the length and orientation of the wavevector (or  $k_x$  and  $k_z$ ), and thus determine the ‘wedge’ on the spectral lattice (Figure 1a), i.e., the spectral support of the curvelet. Each particular wedge, in turn, defines a dual spatial lattice (Figure 1b). The translation parameters  $k^1$  and  $k^2$  determine the location on this lattice. Overall, curvelets are obtained by anisotropic dilations (remember the anisotropic scaling relation), rotations, and translations of 2D waveforms that are smooth and oscillatory in the one direction and bell-shaped in the orthogonal direction.

Let  $\gamma_{\mu_u}$  be a curvelet, with index  $\mu_u = (j, l, k^1, k^2)$ . Using that curvelets are a tight frame, we represent the action of  $\mathcal{H}$  in terms of  $\gamma_{\mu_u}$  as

$$\langle \gamma_{\mu_m}, \mathcal{H}u \rangle = \sum_{\mu_u} \mathcal{H}_{\mu_m \mu_u} \langle \gamma_{\mu_u}, u \rangle, \quad (1)$$

### Constructing the inverse scattering operator

Let  $\mathcal{F}$  be the modeling or scattering operator. The geometry of the action of this operator and its adjoint  $\mathcal{F}^*$ , the imaging operator, is described by its canonical relation  $\Lambda$ , which relates the data (reflection positions, traveltimes and slopes) to the image (location and orientation of the imaged reflectors). Under some weak conditions,  $\mathcal{F}$  and  $\mathcal{F}^*$  are FIO’s. By composition of  $\mathcal{F}^*$  with an appropriate pseudodifferential operator, e.g.,  $\Xi = (\mathcal{F}^* \mathcal{F})^{-\frac{1}{2}}$ , we obtain a continuous inverse scattering operator  $\mathcal{H} = \Xi \mathcal{F}^* : L^2(Y) \mapsto L^2(X)$ , where  $Y$  contains the acquisition variables and  $X$  the scattering points. In this case,  $\mathcal{H}$  is a continuous FIO of order zero. This operator belongs to the class of FIO’s that are optimally sparsified by curvelets. A key condition for the decomposition of FIO’s is that the canonical relation  $\Lambda$  be a canonical graph. In that case, the situation that a single surface seismic measurement has multiple images cannot occur. Since curvelets are currently 2D, we will limit ourselves to 2D seismics.

### Inverse scattering in the curvelet domain

Wavelets sparsify objects with point singularities well, but fail to sparsify objects with edges along curves. It turns out that such edges can be represented by a superposition of functions of different lengths and widths that satisfy the anisotropic scaling relation  $width \approx length^2$ . These functions are called *curvelets*. The upper left panel in Figure 2 shows an example of a curvelet.

Roughly speaking [for details see Candès and Guo (2002) and Candès and Donoho (2002)], curvelets are 2D extensions of wavelets. Just as wavelets are localized in one variable and its Fourier dual (e.g., time and frequency), curvelets are localized in two variables and their Fourier duals (e.g., 2D space and 2D spectrum). Thus, much as wavelets are determined by a tiling of, e.g., the time-frequency plane, curvelets are determined by a tiling of, e.g., both the  $x$ - $z$  plane and its 2D spectrum (Figure 1 shows the tiling of these planes for the digital curvelet transform we use throughout this work). Therefore, just as wavelets are determined by two parameters (scale and translation), curvelets are determined by four parameters,

where the matrix  $\mathcal{H}_{\mu_m \mu_u} = \langle \gamma_{\mu_m}, \mathcal{H} \gamma_{\mu_u} \rangle$ ,  $u$  is the recorded wavefield, and  $\gamma_{\mu_u}$  and  $\gamma_{\mu_m}$  are the curvelets in the data and image domain respectively, i.e.,  $\mu_u$  and  $\mu_m$  are the indices related to the (unmigrated) data and (migrated) image domain. The mapping of  $\mu_u$  to  $\mu_m$  is governed by map migration. To prove the concept just outlined, we restrict ourselves throughout the remainder of this work to CO Kirchhoff migration in the absence of caustics.

### CO curvelet time-migration

Recently, Douma and de Hoop (2003) derived explicit expressions for CO map time-migration. The 2D expressions are easily derived from their 3D counterparts [equations (7), (8) and (11) in Douma and de Hoop (2003)] and provide us with  $x_m(x_u, t_u, p_u, h, v)$ ,  $t_m(x_u, t_u, p_u, h, v)$ , and  $p_m(x_u, t_u, p_u, h, v)$ , where  $x_u$ ,  $t_u$ , and  $p_u = \frac{1}{2} \frac{\partial t_u}{\partial x_u}$  are the midpoint location, two-way (unmigrated) traveltime, and the (unmigrated) slope in a CO section respectively,  $x_m$ ,  $t_m$  and  $p_m = \frac{1}{2} \frac{\partial t_m}{\partial x_m}$  are the migrated location, two-way traveltime and slope respectively,  $h$  is the half-offset, and  $v$  is the medium velocity. These expressions define the canonical relation (from the unmigrated quantities to their migrated counterparts) for 2D CO Kirchhoff time-migration, which is given by

$$\Lambda = \{(x_u, t_u, \omega p_u, \omega; x_m, \xi_m)\}, \quad (2)$$

with  $x_m = (x_u, vt_m/2)$  the migrated location, and  $\xi_m = (|\xi_m| \sin \theta_m, -|\xi_m| \cos \theta_m)$  the wavevector associated with the reflector ( $\theta_m$  is the angle measured clockwise positive with the downward vertical). The angle of this wavevector is related to  $p_m$  as  $\theta_m = \tan^{-1}(vp_m)$ , while its length  $|\xi_m|$  is given by

$$|\xi_m| = \frac{\omega}{v} \cos\left(\frac{\theta_r - \theta_s}{2}\right), \quad (3)$$

with  $\theta_s = \tan^{-1}[2(x_u - h - x_m)/(vt_m)]$  and  $\theta_r = \tan^{-1}[2(x_u + h - x_m)/(vt_m)]$ .

Now, we follow the work of Candès and Demanet (2002) and show that  $\Lambda$  indeed defines the mapping from  $\mu_u$  to

## Pre-stack map migration with curvelets

$\mu_m$ . Let  $\gamma_{\mu_u}$  be a curvelet with scale  $2^{-j_{\mu_u}}$ , phase direction  $\theta_{\mu}$  (or orientation parameter  $l_{\mu_u}$ ), and location  $x_{\mu_u}$  (or translation parameters  $k_{\mu_u}^1$  and  $k_{\mu_u}^2$ ). The scale determines the length of the unmigrated wavevector  $\xi_u$  and thus the dominant frequency  $\omega$  of the curvelet. The phase direction  $\theta_{\mu}$  is related to the unmigrated slope as  $p_u = \tan \theta_{\mu}/v$ , while the location  $x_{\mu_u} = (x_u, vt_u/2)$ . Hence, we have all the necessary information (i.e.,  $x_u$ ,  $t_u$ ,  $p_u$  and  $\omega$ ) to use  $\Lambda$  to find the migrated location ( $x_m$ ) and wavevector ( $\xi_m$ ) in the image. To determine  $\mu_m$ , we find the wedge in the spectral lattice that contains the endpoint of  $\xi_m$ , and the cell in the spatial lattice that contains the migrated location. This wedge in the spectral lattice determines the scale and the orientation parameters  $j_{\mu_m}$  and  $l_{\mu_m}$  of the migrated curvelet, while the cell in the spatial lattice determines its translation parameters  $k_{\mu_m}^1$  and  $k_{\mu_m}^2$ . Note that the scale parameter  $j_{\mu_u}$  can be different from  $j_{\mu_m}$ , since in general  $|\xi_u| \neq |\xi_m|$ . The pairing of  $\mu_u$  and  $\mu_m$  found in this way, describes the geometry of the migration.

### Example

In order to estimate what becomes of a curvelet after subjecting it to migration, we CO Kirchhoff time-migrate a curvelet and examine the coefficients of the resulting output in the curvelet frame. Herrmann (2003) also migrated (and demigrated) curvelets, and observed that “they remain fairly localized”. Here, we use the coefficients of CO Kirchhoff migrated curvelet for a comparison with the migrated curvelet coefficients resulting from our map migration.

The top row of Figure 2 shows, from left to right, a curvelet in space (we converted the time axis to depth,  $z = vt_u/2$ , for consistency with the remaining figures), its coefficients on the spatial lattice, and its spectrum. The coefficients for this curvelet are shown on the spatial lattice (the grid shown in the middle panel); each cell in this lattice, which is related to the translation parameters  $k^1$  and  $k^2$ , is shaded according to the normalized absolute values of the coefficients (black equals one and white equals zero).

The middle row shows the result after subjecting the curvelet in the top row of Figure 2 to a 2D CO Kirchhoff time-migration. Here we used  $v = 3.0$  km/s and  $h = 1$  km. Notice how the migrated curvelet determines only *part* of the isochron (indicated by the dashed line). This is in sharp contrast to the resulting *whole* isochron if we would migrate a single spike, the basis function currently used to represent seismic data. The (nonzero part of the) spectrum of the migrated curvelet overlaps several wedges in the spectral lattice, indicating that the migration induces some leakage into neighboring curvelets. The main energy, however, resides in the wedge labeled ‘1’. The middle panel shows the coefficients for the spatial area in the lower left quadrant of the leftmost figure (outlined by the dotted lines), for the wedges labeled ‘1’ through ‘4’. Indeed there is also some leakage to neighboring curvelets in space, but again this can be considered small. Ideally, we would like to see no such leakage, and have a single curvelet on output after migrating one curvelet. In that case we could image seismic data by mapping curvelets one for one, without any loss of accuracy. The fact that we observe little leakage indicates that the curvelet frame approaches this situation.

The bottom row shows the result of CO map time-migrating the curvelet from the top row, using the mapping outlined above. Indeed the map-migration finds the wedge that had the most energy after the Kirchhoff migration (labeled ‘1’), while the translation parameters from the map-migration identify the cell in the spatial lattice that lies next to the cell with the maximum coefficient after the Kirchhoff migration (see the middle panel of the bottom row in Figure 2). Thus, map-migration identifies the index  $\mu_m$  near the indices of the largest coefficients of  $\mathcal{H}\gamma_{\mu_u}$ . This is precisely the behavior of the action of an FIO on curvelet elements predicted by Candès and Demanet (2002). Hence, using curvelets, we have built a wave-character preserving pre-stack map time-migration. Significantly, in our example, the map time-migration with curvelets is almost two orders of magnitude faster than the Kirchhoff migration.

### Conclusions

We argue that curvelets are plausible candidates for simultaneous sparsification of seismic data and the inverse scattering operator, and treat the decomposition of this operator in the curvelet frame. In addition we state the conditions under which sparsification of this operator is feasible. Knowing that CO Kirchhoff migration in the absence of caustics satisfies these conditions, we analyze the sparsity after CO Kirchhoff time-migrating a curvelet, and observe little leakage into neighboring curvelets, in both the spatial and spectral domains. This exemplifies the ability of curvelets to sparsify the imaging operator.

A comparison of a CO Kirchhoff time-migrated curvelet with a CO map time-migrated curvelet shows that map migration maps the indices of the unmigrated curvelets onto (or near) the indices of the largest coefficients of the migrated curvelets. Therefore, map migration indeed provides the geometry of the migration in the curvelet domain. Hence, we can devise a wave-character preserving map migration that in essence images the data in the compressed domain through a mapping of coefficients. In essence, we present the CO time-migration variant of this, albeit we do not treat the amplitude aspects of the imaging, as this still requires a technical analysis. The CO curvelet time-migration we present can readily be used for time-migration velocity analysis. Significantly, the wave-character preserving CO map time-migration, here, is almost two orders of magnitude faster than the CO Kirchhoff migration.

### Acknowledgements

We thank Emmanuel Candès for providing us with his Matlab implementation of the digital curvelet transform via unequally spaced Fourier transforms, and for invaluable discussions, and Ken Larner for his careful review of this abstract. The support for this work was provided by the Consortium Project on Seismic Inverse Methods for Complex Structures at CWP. H.D. acknowledges the partial financial personal support of WesternGeco.

### References

Boutet de Monvel, L., 1974, Hypoelliptic operators with

## Pre-stack map migration with curvelets

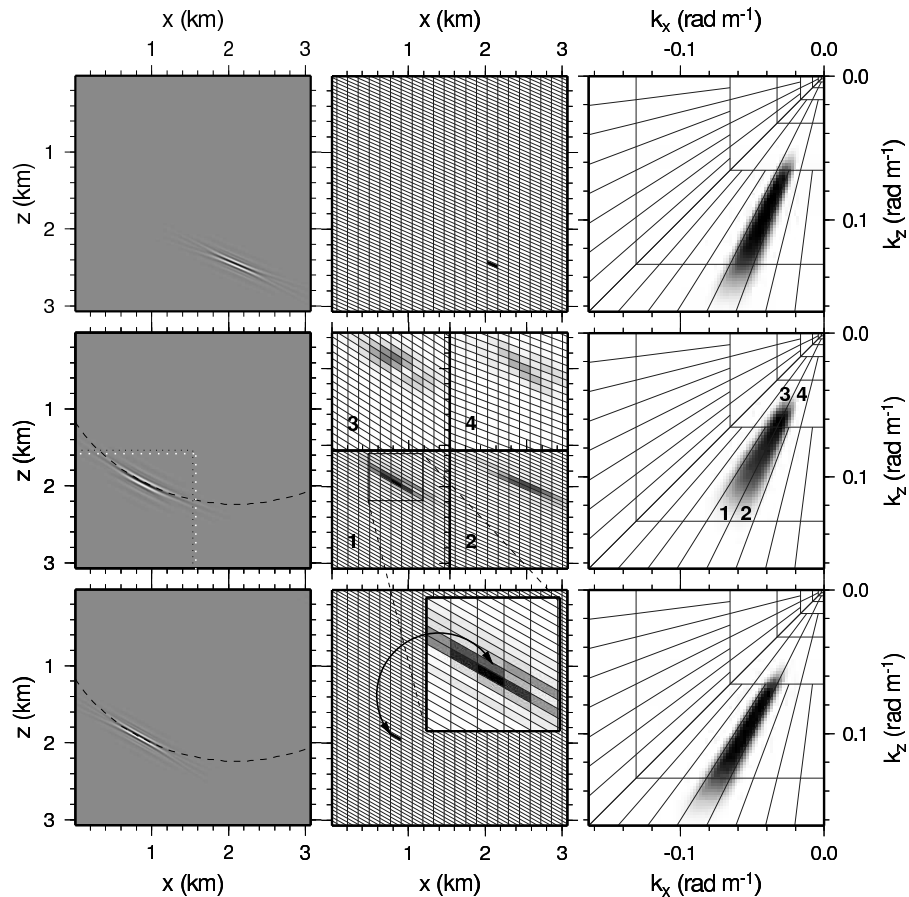


Fig. 2: Comparison between CO Kirchhoff time migration and CO map time-migration with curvelets. The top row shows a curvelet with a dominant frequency of about 30 Hz (left, shown in depth,  $z = vt_u/2$ , for consistency), the normalized absolute values of the coefficients on the spatial lattice (middle), and its spectrum (right). The middle row shows the CO Kirchhoff migration of the curvelet in the top row. The middle panel in this row shows the coefficients on the spatial lattice in the lower left quadrant of the leftmost panel (indicated with the dotted lines in the leftmost panel) for each of the numbered wedges (labeled '1' to '4') in the spectrum (right). The bottom row shows the result from CO map time-migration.

- double characteristics and related pseudodifferential operators: *Comm. Pure Appl. Math.*, **27**, 585–639.
- Candès, E. J., and Demanet, L., 2002, Curvelets and Fourier integral operators: To appear in *Comptes-Rendus de l'Academie des Sciences, Paris, Serie I*.
- Candès, E. J., and Donoho, D. L., 2002, New tight frames of curvelets and optimal representations of objects with  $C^2$  singularities: Technical Report, Stanford, *submitted*.
- Candès, E. J., and Guo, F., 2002, New multiscale transforms, minimum total variation synthesis: Applications to edge-preserving image reconstruction: *Signal Processing*, **82**, 1519–1543.
- Douma, H., and de Hoop, M. V., 2003, Explicit expressions for pre-stack map time-migration in isotropic and VTI media and the applicability of map depth-migration in heterogeneous anisotropic media: *Accepted for publication in Geophysics*.
- Gjoystdal, H., and Ursin, B., 1981, Inversion of reflection times in three dimensions: *Geophysics*, **46**, 972–983.
- Herrmann, F., 2003, Optimal imaging with curvelets: Annual meeting of the SEG, Expanded Abstracts.
- Hua, B., and McMechan, G. A., 2003, Parsimonious 2D prestack Kirchhoff depth migration: *Geophysics*, **68**, 1043–1051.
- Iversen, E., Gjoystdal, H., and Hansen, J., 2000, Prestack map migration as an engine for parameter estimation in TI media: 70th Ann. Internat. Mtg. Soc. of Expl. Geophys., pages 1004–1007.
- Kleyn, A., 1977, On the migration of reflection time contour maps: *Geophysical Prospecting*, **25**, 125–140.
- Smith, H., 1998, A parametrix construction for wave equations with  $C^{1,1}$  coefficients: *Ann. Inst. Fourier*, **48**, 797–835.